01 Jul 1990

Mössbauer-Effect, Magnetic, and Neutron-Diffraction Study of $NaFeP_2O_7$

R. C. Mercader

L. Terminiello

Gary J. Long
Missouri University of Science and Technology, glong@mst.edu

D. G. Reichel

et. al. For a complete list of authors, see https://scholarsmine.mst.edu/chem_facwork/917

Recommended Citation

R. C. Mercader et al., "Mössbauer-Effect, Magnetic, and Neutron-Diffraction Study of $NaFeP_2O_7$," *Physical Review B*, vol. 42, no. 1, pp. 25-32, American Physical Society (APS), Jul 1990.
The definitive version is available at https://doi.org/10.1103/PhysRevB.42.25

Mössbauer-effect, magnetic, and neutron-diffraction study of $NaFeP_2O_7$

R. C. Mercader* and L. Terminiello
Departamento de Fisica, Universidad Nacional de La Plata, 115 y 49, 1900 La Plata, Argentina

Gary J. Long*
Department of Chemistry, University of Missouri–Rolla, Rolla, Missouri 65401-0249

D. G. Reichel and K. Dickhaus
University of Missouri, Research Reactor, Columbia, Missouri 65211

R. Zysler, R. Sanchez, and M. Tovar
Centro Atomico Bariloche and Instituto Balseiro, 8400 Bariloche, Rio Negro, Argentina
(Received 25 January 1990)

Neutron-diffraction, magnetic-susceptibility, specific-heat, and Mössbauer-effect studies of $NaFeP_2O_7$ reveal that it is a normal Heisenberg isotropic three-dimensional antiferromagnetic material with a Néel temperature of 29.0 K. $NaFeP_2O_7$ has the monoclinic $P2_1/c$ magnetic space group, which is the same as the nuclear crystallographic space group. The easy axis of magnetization lies in the monoclinic *ac* plane at an angle of 21.0° from the *c* axis. The specific-heat measurements reveal a λ-type anomaly at 28.7(2) K. A molecular-field model analysis indicates that the intrasublattice magnetic exchange coupling $J_{aa}=J_{bb}=-0.37$ cm^{-1}, whereas the intersublattice coupling $J_{ab}=-0.61$ cm^{-1}. No evidence for *L*-type ferrimagnetism is observed.

I. INTRODUCTION

The relevance of the interplay between exchange interactions and crystallographic structure is evident in a recent series of studies of the magnetic properties of anhydrous Fe(III) sulfate,[1] $Fe_2(SO_4)_3$, Fe(III) molybdate,[2] $Fe_2(MoO_4)_3$, synthetic langbeinite,[3] $KBaFe_2(PO_4)_3$, and Fe(III) tungstate,[4] $Fe_2(WO_4)_3$. All these compounds contain FeO_6 octahedra sharing corners with MO_4 tetrahedra, where *M* is sulfur, molybdenum, phosphorous, or tungsten. For these structures the cyrstallographically inequivalent iron sites display different temperature dependences for the molecular field, giving rise to *L*-type ferrimagnetism.[1–5] The structure of $NaFeP_2O_7$ contains coordination polyhedra chains similar to those described above. Due to the structural similarities between $NaFeP_2O_7$, $Fe_2(SO_4)_3$, $(MoO_4)_3$, and related materials, *L*-type ferrimagnetism has also been proposed for $NaFeP_2O_7$.[6]

Because an exact solution of the Heisenberg Hamiltonian is intractable even in the simpler cases, some laborious calculations of the superexchange parameters with *ab initio* models have been performed,[7] but with limited success. In addition, it is difficult to evaluate *ab initio* results in view of the many approximations involved. Hence, the semiempirical evaluation[8] of superexchange pathways is important because it provides a framework within which to compare experimental results and predictions made with more elaborate models. Because $NaFeP_2O_7$ contains an octahedrally coordinated high-spin Fe(III) ion with a low distortion of the immediate environment, its magnetic properties are expected to be isotropic and well predicted within the Heisenberg model. Furthermore, its comparison with the preceding compounds permits the study of the influence of the superexchange pathway distance and geometry, and the influence of the electronegativity of the cations on the magnetic behavior. In this paper we report on the magnetic structure and Mössbauer spectral properties of $NaFeP_2O_7$ and present a semiempirical molecular-field analysis of its magnetic exchange.

II. EXPERIMENTAL

Powder samples of $NaFeP_2O_7$ were prepared by firing stoichiometric mixtures of Fe_2O_3, ammonium dihydrogen phosphate, and sodium hydrogen carbonate in a platinum crucible, initially in three 2 h steps, with grinding between each step, from 500 to 1170 K. The sample was held at 1170 K for a total of 8 h with grinding after each 2 h heating interval. Finally, the temperature was raised to 1370 K for an hour and then the sample was slowly cooled to 1170 K at a rate of 10 °C/h, and subsequently air quenched to room temperature.

An x-ray-diffraction analysis of the resulting pink powder at various temperatures indicated that the phase of our sample of $NaFeP_2O_7$ was the same as the monoclinic high-temperature phase reported by Gabelica Robert.[9] No structural changes were observed between 77 and 300 K.

Mössbauer spectra were obtained by using a conventional constant-acceleration spectrometer with 50 mCi ^{57}Co-Rh matrix source which was held at room temperature. The spectrometer was calibrated at room tempera-

ture with natural α-iron foil. A variable-temperature insert placed in a liquid helium cryostat was used to obtain spectra in the range 4.2 to 32 K. A liquid nitrogen cryostat was used for the measurements between 77 and 300 K. The spectra were fit with Lorentzian lines by using a nonlinear least-squares program. Between 4.2 and 26.5 K each spectrum was fit with one magnetic sextet with equal linewidths. One quadrupole doublet was used for the paramagnetic spectra.

The neutron-diffraction patterns of finely powdered samples of $NaFeP_2O_7$ were measured in a vanadium sample holder with the position-sensitive detector diffractometer at the University of Missouri Research Reactor. A closed-cycle refrigerator was used for measurements at 40, 20, and 8 K. Data were collected in three spans from 10 to 90° in 2ϕ in approximately 24 h at each temperature. The data were rebinned into 0.1° steps resulting in 800 data points. The data were analyzed by using a modified Rietveld code including a Voigt function to describe a mixed Gaussian-Lorentzian line shape for the peaks.

Magnetic-susceptibility measurements were performed by using a Faraday balance operating in the temperature range from 2 to 300 K. Specific-heat measurements were made with a semiadiabatic calorimeter. The sample was powdered and thoroughly mixed with a conducting grease[10] in a one to one proportion in order to improve the thermal conductivity of the sample.

III. MAGNETIC-SUSCEPTIBILITY RESULTS

The magnetization of powdered samples of $NaFeP_2O_7$ was found to be linear with the applied magnetic field up to 1 T. The corresponding magnetic susceptibility, $\chi_M = \partial M / \partial H$, follows a Curie-Weiss law above ~ 30 K, as is shown in Fig. 1. The effective magnetic moment of $5.93(3)\mu_B$/ Fe atom, determined after correction for the core diamagnetism, is constant between 30 and 300 K. This value is closer to the $5.92\mu_b$/Fe value expected for a high-spin iron(III) compound than is the value of $5.60\mu_B$/Fe atom found by Moya-Pizarro *et al.*[6] The Curie-Weiss temperature of $\Theta = 53.4(1)$ K indicates antiferromagnetic interactions. At temperatures below 28.5 K a very small remnant magnetization develops and reaches a maximum value of $0.0124\mu_B$/Fe atom at 2 K, as is shown in Fig. 2. In this temperature range the magnetic susceptibility remains approximately constant. This behavior is characteristic of an antiferromagnetic compound with a weak ferromagnetic component. This component corresponds to a slight misalignment of the magnetization of the sublattices of $\sim 0.2°$ and might arise either from a Dzyaloshinskii-Moriya interaction or single ion magnetocrystalline anisotropy.[11] From these data we find a Néel temperature $T_N = 28.5(5)$ K.

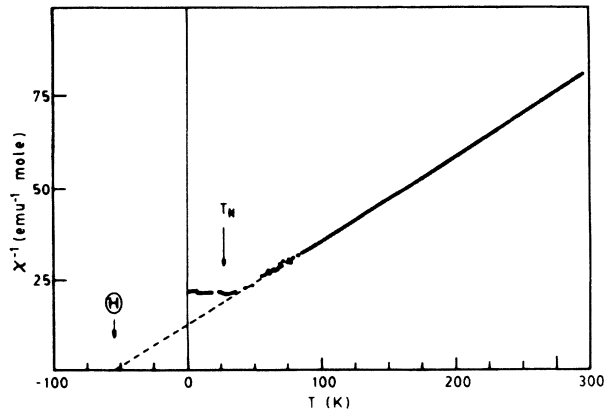

FIG. 1. The inverse magnetic susceptibility of $NaFeP_2O_7$.

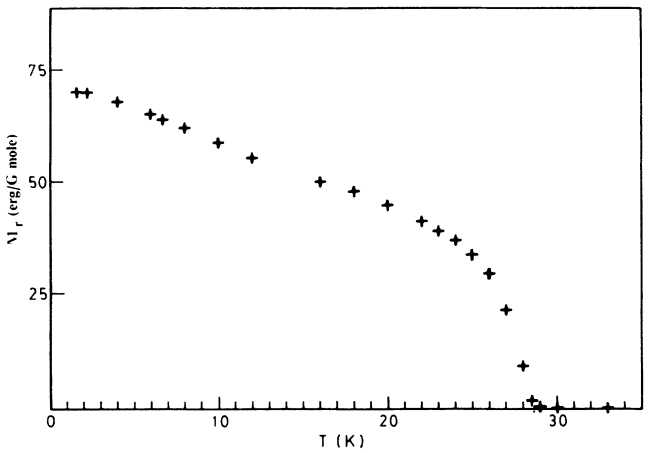

FIG. 2. The remnant magnetization in $NaFeP_2O_7$.

IV. NEUTRON-DIFFRACTION DATA REFINEMENT

The Rietveld refinement was initiated with the 300 K data and used the results of a single crystal x-ray study of $NaFeP_2O_7$ published by Gabelica-Robert *et al.*[9] Our refinement, after a linear subtraction of the incoherent background scattering, lead to an immediate refinement of the nuclear structure with the resulting crystallographic and refinement parameters presented in Table I. The resulting positional parameters at 300 and 8 K are given in Table II. In this refinement, in the monoclinic $P2_1/c$ space group, the overall scale factor, three half-width parameters, a Voigt profile parameter, the zero point, a preferred orientation parameter, an asymmetry parameter, four crystallographic cell constants, 33 atomic positional parameters, and four isotropic thermal parameters, for a total of 49 parameters, were adjusted. The thermal parameters were fixed to the same value (see Table I) for the two phosphorus atoms and for all the oxygen atoms. The results of this refinement are shown in Fig. 3, which reveals an excellent agreement between the experimental data points and the calculated Rietveld diffraction profile. There was no evidence of any magnetic scattering at 300 K.

The experimental profile measured at 40 K was, except for the reduction in the background incoherent scattering, virtually identical with that obtained at 300 K when the small reduction in the unit cell parameters is taken into account. The refinement of the 40 K data was initiated by using the results obtained at 300 K and im-

TABLE I. Structural and magnetic parameters for $NaFeP_2O_7$.

Temperature (K)	300	40	20	8
Lattice parameters				
a(Å)	7.3116(7)	7.3131(8)	7.3118(8)	7.3116(9)
b(Å)	7.8861(7)	7.8546(8)	7.8533(8)	7.8526(9)
c(Å)	9.5583(9)	9.5594(10)	9.5596(10)	9.5566(12)
β (deg)	111.820(7)	111.897(7)	111.903(8)	111.895(9)
V(Å^3)	511.65(10)	509.49(12)	509.30(12)	509.11(14)
Isotropic thermal parameters				
B, Na, Å^2	0.54(28)	−0.33(22)	1.34(32)	1.15(24)
B, Fe, Å^2	0.09(7)	0.68(8)	1.04(8)	0.51(10)
B, P, Å^2	0.00(10)	0.40(11)	1.62(24)	0.50(25)
			1.22(23)	−0.64(20)
B, O, Å^2	0.10(04)	0.37(4)	1.00(5)	0.04(5)
Scale factor	0.468(5)	0.390(5)	0.358(3)	0.466(4)
Voigt	394(66)	467(90)	415(74)	962(77)
Zero point, deg	−0.462(4)	−0.029(4)	−0.036(4)	−0.034(4)
Pref. orient. parameters	0.042(8)	−0.003(9)		
R_{nuc}	4.10	3.92	4.77	3.47
R_{mag}			22.8	5.18
χ^2	2.3	3.2	3.5	4.2
NDF	759	754	771	771
Magnetic parameters[a]				
K_a			−0.04(37)	1.68(17)
K_b			0.00	0.00
K_c			1.14(17)	4.68(6)
Moment, μ_B			1.16(11)	4.35(6)

[a] The magnetic rotation matrices are (100,010,001), (−100, 0+10, 00−1), (100,010,001), and (−100,0+10,00−1).

mediately converged to the same structure as revealed by the results presented in Tables I and II. There was no evidence of any magnetic scattering in the experimental neutron-diffraction results at 40 K.

The resulting structure is virtually identical to that reported by Gabelica-Robert *et al.*[9] and Moya-Pizarro *et al.*[6] and, as usual, the neutron-diffraction lattice parameters are better determined than the x-ray lattice parameters and are almost the average of those reported earlier.[6,9] It is interesting that there is only a 0.5 percent reduction in the unit cell volume between 300 and 8 K; the decrease occurring predominantly along the unique monoclinic b axis. Strangely the observed thermal parameters increase upon cooling. This increase presumably is an artifact of the baseline correction procedure. There is a strong correlation between the baseline and the thermal parameters.

The powder neutron-diffraction patterns obtained at 8 [see Fig. 3(b)] and 20 K, and hence below the magnetic ordering temperature show, in addition to the expected nuclear scattering, magnetic scattering at the 010 and 101 reflections, reflections for which the nuclear scattering is forbidden in the $P2_1/c$ space group. The additional magnetic scattering is easily seen in Fig. 3(b) which shows intense magnetic scattering at $\sim 11°$ in 2Θ; scattering that is essentially absent in Fig. 3(a) which was obtained above

TABLE II. Positional parameters for $NaFeP_2O_7$.

	300 K			8K		
Atom	x	y	z	x	y	z
Na	0.289(2)	0.473(2)	0.300(1)	0.282(2)	0.473(2)	0.299(1)
Fe	0.261(1)	0.008(1)	0.248(1)	0.263(1)	0.006(1)	0.247(1)
P(1)	0.078(2)	0.251(1)	0.458(1)	0.076(2)	0.255(2)	0.456(1)
P(2)	0.674(1)	0.212(1)	0.453(1)	0.681(2)	0.212(2)	0.455(1)
O(1)	0.876(1)	0.153(1)	0.441(1)	0.874(2)	0.154(1)	0.438(1)
O(2)	0.191(2)	0.287(1)	0.620(1)	0.186(2)	0.288(2)	0.620(1)
O(3)	0.014(1)	0.416(1)	0.364(1)	0.006(2)	0.426(1)	0.359(1)
O(4)	0.185(1)	0.133(1)	0.397(1)	0.181(2)	0.142(1)	0.394(1)
O(5)	0.530(1)	0.087(1)	0.352(1)	0.537(2)	0.095(2)	0.355(1)
O(6)	0.694(1)	0.205(1)	0.619(1)	0.694(2)	0.208(2)	0.620(1)
O(7)	0.635(1)	0.394(1)	0.396(1)	0.637(2)	0.393(1)	0.396(1)

the magnetic ordering temperature.

In order to establish the magnetic space group, refinements were performed with magnetic matrices belonging to the possible Shubnikov groups consistent with the experimental evidence arising from other techniques. The analysis of the results indicated that, in order to account for the observed antiferromagnetism, the magnetic moment component parallel to the unique b axis must be set equal to zero. The only reasonable fit was found to belong, like the nuclear scattering, to the $P2_1/c$ space group. Within this magnetic space group the magnetic structure converged immediately to that shown in Fig. 4.

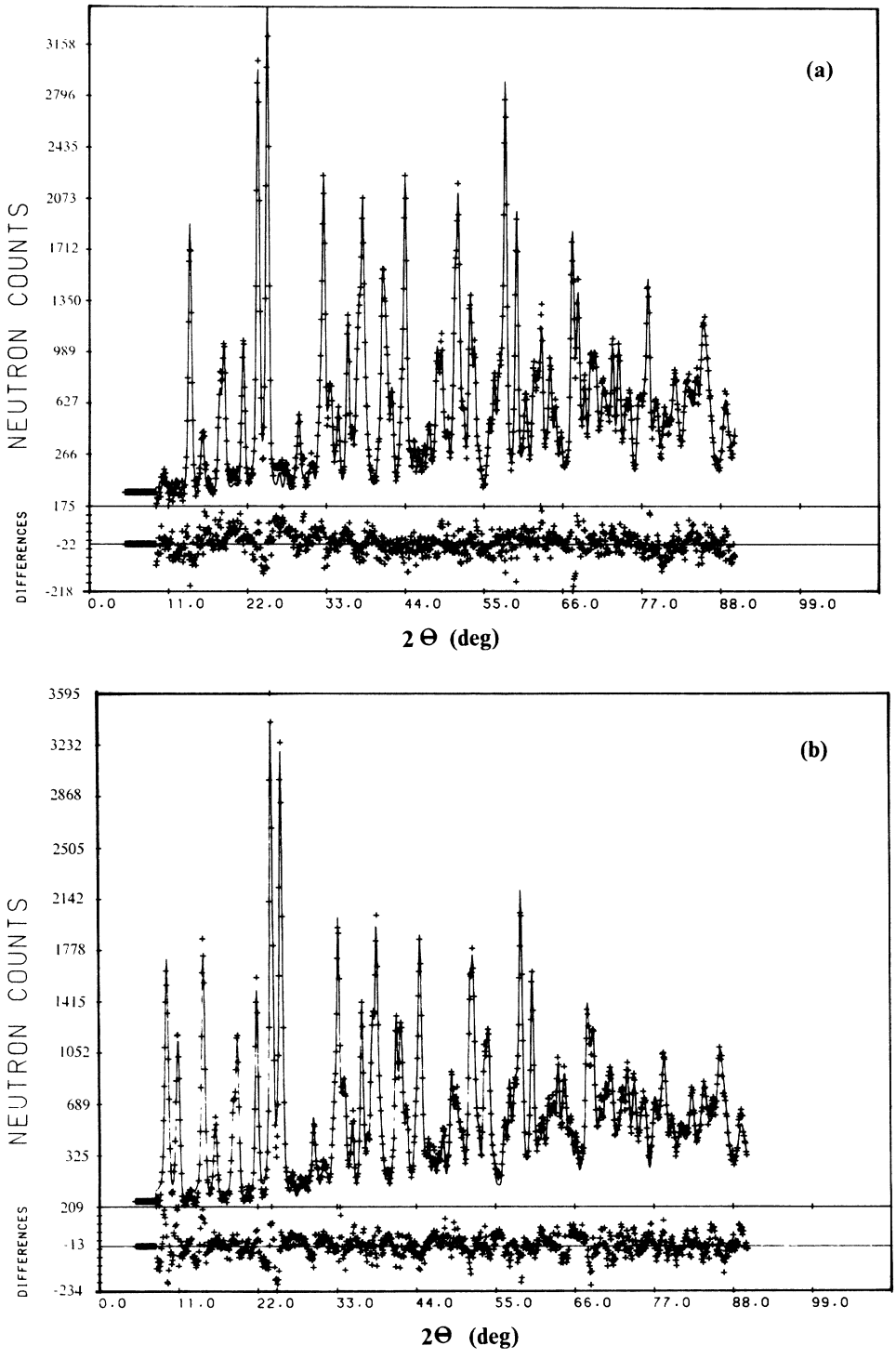

FIG. 3. Powder neutron-diffraction pattern obtained for $NaFeP_2O_7$ at 300 K (a) and 8 K (b). The solid line represents the Rietveld line profile analysis discussed in the text.

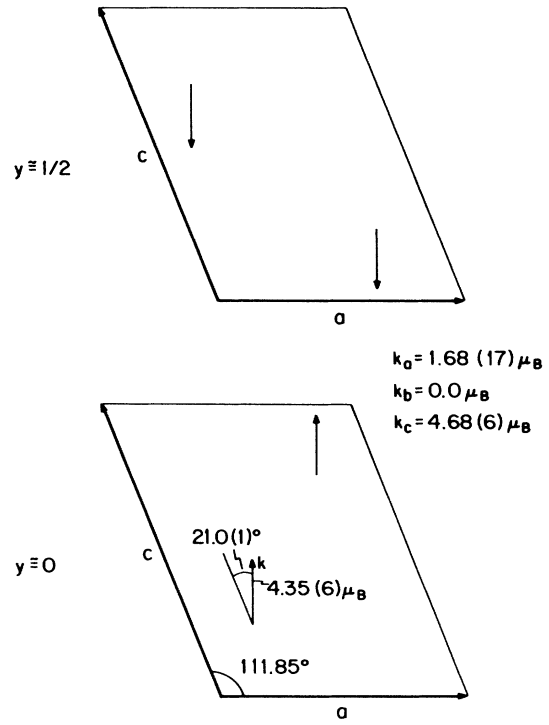

FIG. 4. The orientation of the easy axis of magnetization in $NaFeP_2O_7$.

The resulting components of the magnetic moments along the crystallographic axis and the resultant moment are given in Table I. The results clearly indicate that $NaFeP_2O_7$ is antiferromagnetic with the easy axis of magnetization at 21.0(1) degrees from the c axis as is shown in Fig. 4.

V. MÖSSBAUER SPECTRAL RESULTS

The Mössbauer spectra of $NaFeP_2O_7$, obtained at several temperatures between 32 and 4.2 K, are shown in Fig. 5. Two types of spectra were observed, indicating different magnetic regimes. Below ~29 K magnetically ordered spectra were observed, whereas above this temperature, paramagnetic spectra were observed. Between 4.2 and 28.5 K each spectrum was fit with one magnetic sextet with equal linewidths. At 26.5 and 28.5 K different linewidths were required to fit the sextets, either because of relaxation broadening near the magnetic ordering temperatures or a sample inhomogeneity, which leads to a "smearing" of the phase transition with temperature. The resulting hyperfine spectral parameters, corresponding to the fits shown in Fig. 5, are given in Table III. All spectra observed between 300 and 32 K exhibit an unresolved quadrupole doublet as illustrated in Fig. 5 at 32 K. This is a clear demonstration of paramagnetic behavior at 32 K and above and a transition to an ordered antiferromagnetic phase, found by neutron diffraction and magnetic studies, at temperatures below $T_N = 29.0(5)$ K. The quadrupole doublet paramagnetic spectra reveal the presence of a small electric-field gradient at the iron (III) site as expected for the small distortion observed in the

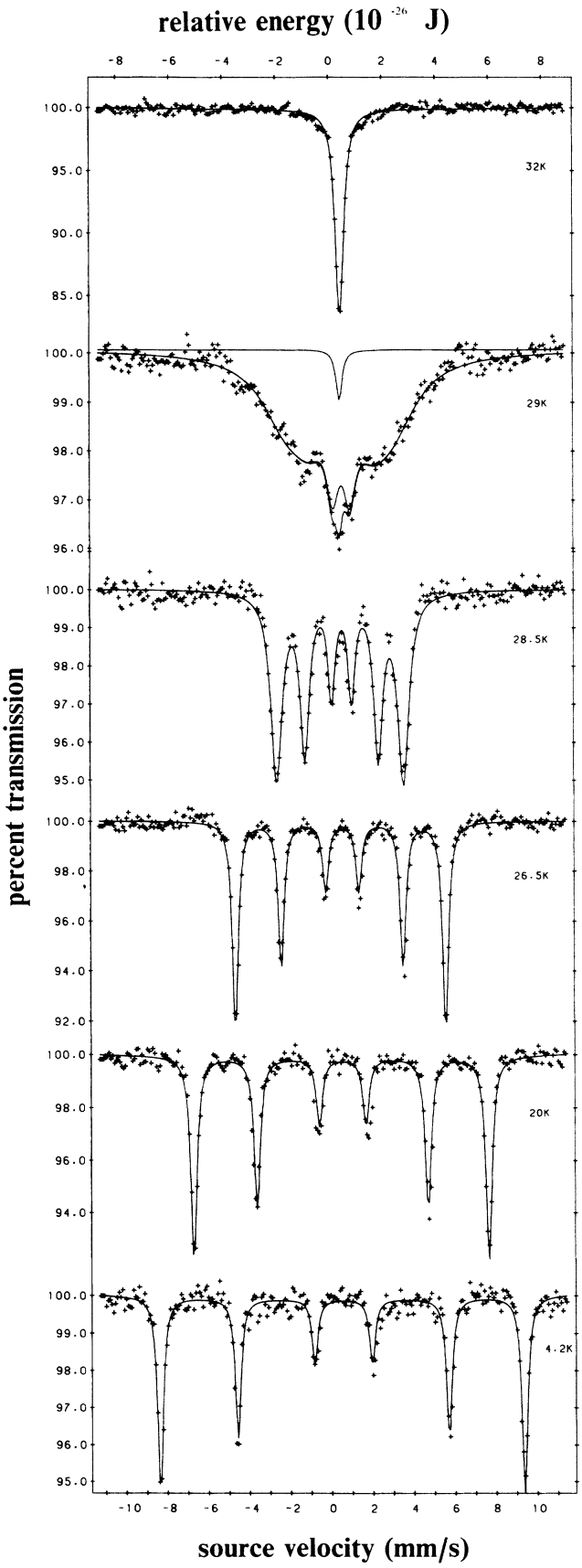

FIG. 5. The Mössbauer spectra of $NaFeP_2O_7$ obtained at various temperatures.

TABLE III. Mössbauer effect hyperfine parameters for $NaFeP_2O_7$.

T K	H_{int} kOe	δ[a] mm/s	QS mm/s	Γ mm/s	$A^b_{2/5}$
4.2	549	0.54	-0.06	0.33	2.11
5.0	549	0.54	-0.06	0.39	2.18
10.0	533	0.54	-0.06	0.31	2.04
20.0	445	0.53	-0.07	0.36	2.23
25.0	370	0.53	-0.08	0.32	2.02
26.5	317	0.54	-0.09	0.35	2.09
28.5	191	0.54	-0.07	0.40	2.03
29.0	161	0.55	-0.07	0.74[c]	2.00
32.0		0.55	0.12[d]	0.46	
295		0.44	0.14[d]	0.29	

[a] Relative to room temperature natural α-iron foil.
[b] The area of the 2, 5 lines in the magnetic sextet.
[c] The outer lines are broadened considerably by relaxation.
[d] The quadrupole interaction in the paramagnetic spectra.

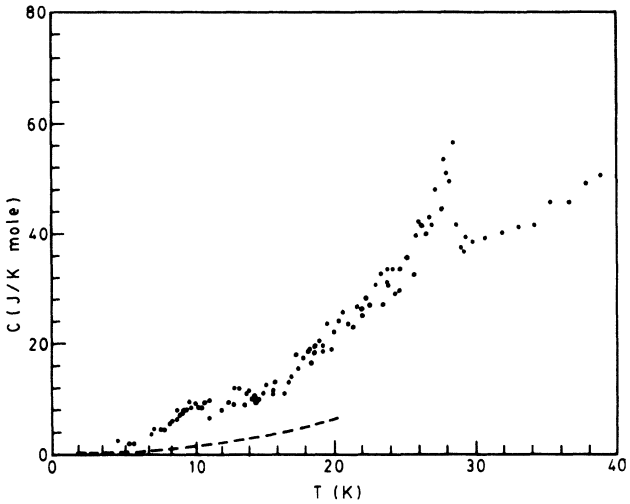

FIG. 6. Specfic heat of $NaFeP_2O_7$. The dashed line corresponds to the specific heat of the cryocon grease.

octahedral coordination environment. The quadrupole splitting, ΔE_Q, is essentially constant above T_N with a value of 0.14(1) mm/s and a linewidth of 0.29(1) mm/s. These values are in excellent agreement with those reported earlier by Moya-Pizarro *et al.*[6] and are typical of an $^6A_{1g}$ electronic ground state. The room-temperature isomer shift of 0.435(5) mm/s is in good agreement with the isomer shifts of similar coordination polyhedra and is representative of paramagnetic high-spin iron(III) in an octahedral crystal field.

Below T_N the compound is magnetically ordered. It was possible to fit the data with a single magnetic sextet of equal linewidths from 4.2 to 26.5 K. At 29 K the impending transition to the paramagnetic state broadens the sextet and a single linewidth fails to give good fits. Within the ordered phase the quadrupole shift remains unchanged at $-0.05(1)$ mm/s, indicating that, unlike anhydrous Fe(III) phosphate, $FePO_4$,[12] $NaFeP_2O_7$ does not undergo a spin rotation. Assuming a zero asymmetry parameter η on the basis of the very small distortion of the FeO_6 octahedra, a value of $60 \pm 10°$ can be derived for the angle between V_{ZZ} and H_{int}. The relative intensities of lines 2 (and 5) to line 3 (and 4) for spectra below 26.5 K gave on average a value of 2.11(8), close to that expected of a randomly oriented powder (3:2:1:1:2:3) and indicating little preferred orientation of the microcrystals as occurred with anhydrous iron (III) sulfate.

VI. SPECIFIC-HEAT MEASUREMENTS

The specific heat was measured from 2 to ~50 K. A λ-type anomaly is observed with a jump in the specific heat at 28.7(2) K as is shown in Fig. 6. No attempt was made to separate the magnetic contribution to the specific heat because both the phonon contribution of $NaFeP_2O_7$ and the high-temperature specific heat of the grease are unknown. The dashed line shown in Fig. 6 is the contribution of the grease up to 20 K and has been included for comparison. A value of $C/R = 2.4(3)$ could be estimated for the specific-heat jump at T_N which is consistent with a mean-field calculation for an S equal to $\frac{5}{2}$ magnetic state.

VII. MAGNETIC ORDERING MODEL

In $NaFeP_2O_7$ each Fe(III) ion is coordinated to six oxygen ions from six different pyrophosphate groups. These FeO_6 octahedra are crystallographically equivalent but have two different spacial orientations. As indicated by the neutron-diffraction results, these two classes of differently oriented octahedra correspond to the two antiferromagnetic sublattices. Each magnetic ion is connected to 10 different magnetic neighbors through

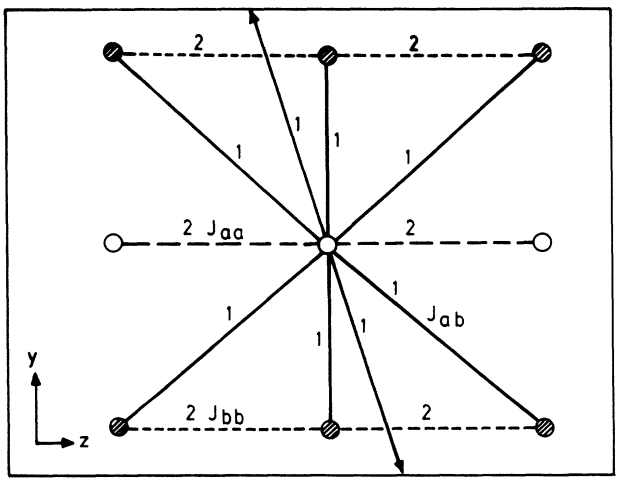

O Fe(1) ● Fe(2)

FIG. 7. A projection of the $NaFeP_2O_7$ atomic coordinates showing the various superexchange pathways.

12 Fe-O-P-O-Fe bridges as is illustrated in Fig. 7. Eight of the 12 bridges are connections to the opposite magnetic sublattice. The four remaining bridges connect the central magnetic ion to two magnetic ions on the same sublattice. Hence there are two double exchange pathways on the same sublattice. In fact, these two double pathways and four of the eight pathways connecting to the opposite sublattice are identical. The only difference in the intrasublattice and intersublattice exchange constants must reside in the four extra pathways connecting each Fe(III) ion to iron ions on the opposite magnetic sublattice.

It seems reasonable that a simple molecular-field model will give a good account of the magnetic properties of $NaFeP_2O_7$ because Fe(III) has a $\frac{5}{2}$ spin state, and when octahedrally coordinated to oxygen, has magnetic properties that are insensitive to small distortions of the octahedron. In order to estimate the exchange interactions responsible for the magnetic ordering in $NaFeP_2O_7$, molecular-field theory has been used to relate the magnetic coupling to the superexchange pathways suggested by the crystalline structure. A similar model has been proposed for monoclinic $Fe_2(SO_4)_3$.[8] By assuming, as expected from the crystallographic studies,[6,9] that the two magnetic sublattices have negligible anisotropy, the molecular-field equations that relate the magnetic field H to the sublattice magnetization $M_0\sigma$ are, in the absence of an applied field,[5]

$$H_a=\lambda_{ab}M_0(-\alpha\sigma_a+\sigma_b)\ , \tag{1}$$

$$H_b=-\lambda_{ab}M_0(\sigma_a-\beta\sigma_b)\ , \tag{2}$$

where λ_{ab} is the intersublattice molecular-field constant, M_0 is the sublattice saturation moment, $g\mu_B N_0 S$, where N_0 is the number of magnetic ions in each sublattice, and μ_B is the electronic Bohr magneton. The intersublattice molecular-field constant is

$$\lambda_{ab}=16J_{ab}/N_0g^2\mu_B^2\ ,$$

where J_{ab} is the intersublattice exchange interaction. The α and β parameters give the relative intensity of the inter to the intrasublattice exchange interaction and are equivalent for $NaFeP_2O_7$. Hence,

$$\alpha=\lambda_{aa}/\lambda_{ab}=J_{aa}/2J_{ab}=\lambda_{bb}/\lambda_{ab}=J_{bb}/2J_{ab}\ ,$$

where J_{aa} and J_{bb} are the average exchange interactions for the two double intersublattice exchange pathways. The exchange interactions are given by the Heisenberg Hamiltonian

$$H_{ij}=-2J_{ij}S_i\cdot S_j\ .$$

The thermal dependence of the sublattice magnetizations are the Brillouin functions

$$\sigma_a=B_s\left[\frac{g\mu_B SH_a}{kT}\right]\ , \tag{3}$$

$$\sigma_b=B_s\left[\frac{g\mu_B SH_b}{kT}\right]\ . \tag{4}$$

The self-consistent solution of Eqs. (1)–(4) will lead to the equilibrium magnetic moment values. The values of λ_{ab} and $\lambda_{aa}=\lambda_{bb}$ are determined by the Curie constant C, the Curie-Weiss temperature θ, and the Néel temperature T_N through the equations

$$\theta=C\lambda_{ab}(1+\alpha)\ ,$$

$$T_N=-C\lambda_{ab}(1-\alpha)\ ,$$

and

$$C=\frac{N_0g^2\mu_B^2S(S+1)}{3k}\ .$$

The values obtained from the susceptibility measurements in the paramagnetic region were used in the molecular-field equations. The values of the exchange interaction resulting from this self-consistent solution are $J_{aa}=J_{bb}=-0.37\ \text{cm}^{-1}$ and $J_{ab}=-0.61\ \text{cm}^{-1}$. These negative values indicate the intrinsic antiferromagnetic nature of the exchange coupling, both within each magnetic sublattice, and between the two sublattices, as was indicated by our preceding analysis of the exchange pathways. The origin of the observed antiferromagnetic coupling no doubt arises from the different number of exchange pathways between sublattices of opposite spin orientation.

The similarity of all angles and distances and the same sign of the intersublattice and intrasublattice exchange interactions are strong evidence for the three-dimensional character of the magnetic ordering. We find no evidence to support the presence of L-type ferrimagnetic interactions as has been proposed earlier.[6]

ACKNOWLEDGMENTS

We thank A. Vasquez, J. B. Marimon da Cunha, and T. Moro of the Mössbauer Laboratory of the Instituto de Fisica, Universidade Federal de Rio Grande do Sul, Porto Alegre, Brasil, for assistance in obtaining the low-temperature Mössbauer data. Further, we thank Dr. G. Punte, Dr. F. Ross, Dr. W. B. Yelon, Dr. O. A. Pringle, Dr. F. Grandjean, and Dr. D. E. Tharp for many helpful discussions during the course of this work. Finally, we thank Consejo Nacional de Investigaciones Científicas y Técnicas (CONICET) of Argentina, Kernforschungszentrum Karlsruhe, Federal Republic of Germany, and the donors of the Petroleum Research Fund, administered by the American Chemical Society, for their support of this research.

*Authors to whom correspondence may be addressed.

[1]G. J. Long, G. Longworth, P. Battle, A. K. Cheetham, R. V. Thundathil, and D. Beveridge, Inorg. Chem. **18**, 624 (1979).

[2]P. D. Battle, A. K. Cheetham, G. J. Long, and G. Longworth, Inorg. Chem. **21**, 4223 (1982).

[3]P. D. Battle, A. K. Cheetham, W. T. A. Harrison, and G. J. Long, J. Solid State Chem. **62**, 16 (1986).

[4]W. T. A. Harrison, P. D. Battle, A. K. Cheetham, and G. J. Long (unpublished).

[5]L. Néel, Ann. Phys. (Paris) **3**, 137 (1948).

[6]T. Moya-Pizarro, R. Salmon, L. Fournes, G. LeFlem, B. Wanklyn, and P. Hagenmuller, J. Solid State Chem. **53**, 387 (1984).

[7]N. L. Huang and R. Orback, Phys. Rev. **154**, 487 (1967); N. L. Huang, *ibid.* **164**, 636 (1967).

[8]J. W. Culvahouse, J. Magn. Magn. Mater. **21**, 133 (1980).

[9]M. Gabelica-Robert, M. Goreaud, P. Labbe, and B. Raveau, J. Solid State Chem. **45**, 389 (1982).

[10]M. S. Toncachvilli, M. N. Yaung, R. Calvo, O. R. Nascimento, and M. B. Maple, Cryogenics **23**, 52 (1983).

[11]C. M. Hurd, Contemp. Phys. **23**, 469 (1982).

[12]P. D. Battle, A. K. Cheetham, C. Gleitzer, W. T. A. Harrison, G. J. Long, and G. Longworth, J. Phys. C **15**, L919 (1982).